Midinfrared intersubband absorption in strain-compensated InGaP/InGaAs superlattices on (001) GaAs

M. P. Semtsiv,[a] G. G. Tarasov, and W. T. Masselink
Department of Physics, Humboldt-Universität zu Berlin, Invalidenstrasse 110, 10115 Berlin, Germany

H. Kissel
Ferdinand-Braun-Institut für Höchstfrequenztechnik, Albert-Einstein-Str. 11, D-12489 Berlin, Germany

M. Woerner
Max-Born-Institut für Nichtlineare Optik und Kurzzeitspektroskopie, D-12489 Berlin, Germany

(Received 6 November 2002; accepted 14 March 2003)

Intersubband optical transitions in strain-compensated $In_{0.32}Ga_{0.68}As-In_{0.32}Ga_{0.68}P$ superlattices grown using gas-source molecular-beam epitaxy on (001)GaAs are investigated by means of midinfrared absorption and low-temperature photoluminescence. Strong absorption corresponding to the transition from the first to second electronic subband is measured at wavelengths between 5.6 and 10.5 μm. The data indicate that the conduction band offset between the strained $In_{0.32}Ga_{0.68}As$ and the strained $In_{0.32}Ga_{0.68}P$ is 370 meV and the electron effective mass in the strained $In_{0.32}Ga_{0.68}As$ well is $0.060m_0$. This material system is an interesting GaAs-based candidate for applications in midinfrared intersubband emitters and detectors. © *2003 American Institute of Physics.* [DOI: 10.1063/1.1573368]

For both optical detectors and emitters operating in the midinfrared part of the spectrum, the use of transitions between the subbands of a quantized conduction band rather than between the conduction and valence bands has a number of advantages. In particular, using intersubband transitions allows the use of wider band gap III–V materials where the transition wavelength is controlled by the structure instead of narrow band gap II–VI or Pb–salt materials where the wavelength is controlled by the material composition. Furthermore, the lifetimes of intersubband excitations are typically significantly shorter than those of interband excitations.[1]

Among the GaAs-based materials, lattice-matched AlGaAs/GaAs, InGaP/GaAs, and In–AlP/GaAs as well as strained AlGaAs/InGaAs material combinations have all found application in intersubband devices; the AlGaAs/GaAs materials system, in particular, has been used both for detectors[2] and quantum cascade lasers (QCLs).[3,4] The maximum conduction band edge offset ΔE_c between direct band gap AlGaAs and GaAs is about 340–390 meV,[5,6] large enough to allow emission wavelengths in QCLs as short as 9 μm.[6] Using strained InGaAs in the wells further increases ΔE_c and extends the emission wavelength range to 7.4 μm.[7] The use of indirect band gap AlGaAs including AlAs, however, does not appreciably increase the maximum emission energy.[8]

An alternative material system which is also lattice matched to GaAs is the strain-compensated (In,Ga)P/(In,Ga)As system,[9] the strain-compensated extension of $In_{0.49}Ga_{0.51}P$/GaAs. Although ΔE_c in the lattice-matched $In_{0.49}Ga_{0.51}P$/GaAs system is too small to use for midinfrared QCL applications, the model-solid theory of Van de Walle[10] predicts a ΔE_c of 480 meV for $In_{0.32}Ga_{0.68}P/In_{0.32}Ga_{0.68}As$, a combination where both materials can be epitaxial deposited and are direct band gap. In the present letter we demonstrate E_1 to E_2 intersubband transitions in $In_{0.32}Ga_{0.68}P/In_{0.32}Ga_{0.68}As$ short-period superlattices up to 220 meV. This result suggests that the strain-compensated (In,Ga)P/(In,Ga)As system may be an attractive candidate for QCL and quantum-well infrared photodetector applications.

Superlattices composed of $In_{0.32}Ga_{0.68}P/In_{0.32}Ga_{0.68}As$ are grown using gas source molecular beam epitaxy semi-insulating GaAs (001) substrates. Following a GaAs buffer layer, the growth temperature is reduced to nominally 350 °C; a low growth temperature is important for maximizing the critical layer thickness for two-dimensional growth in this internally highly-strained system.[11] The InGaP/InGaAs superlattice is then grown at 0.18 nm/s using cracked AsH_3 and PH_3 fluxes of 1.0 and 1.6 sccm, respectively. Because both the InGaP and the InGaAs have the same In and Ga composition, we use single Ga and In effusion cells. (For both the $In_yGa_{1-y}As$ and the $In_yGa_{1-y}P$, the In content is optimized for $0.25 \lesssim y \lesssim 0.35$ so that the barrier is direct, ΔE_c is maximized, and the InGaAs remains pseudomorphic.) During the growth of both materials, the reflection high-energy electron diffraction shows a sharp elemental 1×1 surface reconstruction. To minimize As–P substitution, the switching time between AsH_3 and PH_3 is limited to 1.5 s. Cross-sectional transmission electron microscopy (TEM)[12] shows very uniform and planar layers with no indication of dislocations, islanding, or surface undulations. The internal lattice mismatch values are $\Delta a/a = -1.4\%$ for $In_{0.32}Ga_{0.68}P$ compared to GaAs and $\Delta a/a = +2.4\%$ for $In_{0.32}Ga_{0.68}As$ compared to GaAs. The total mismatch of the strain-compensated structures is as low as 187 ppm. The required occupation of the lowest conduction subband in the InGaAs is achieved by doping the InGaP barriers with Si, resulting in

[a]Electronic mail: semtsiv@physik.hu-berlin.de

TABLE I. Description of samples.

No.	N_{2D} (cm^{-2}/well)	$\mu_{300\,K}$ (cm^2/V s)	L_W (nm)	L_B (nm)	$\Delta a/a$ (ppm)	Periods
A13	2×10^{12}	3900	10.0	12.4	2724	26
A14	1.4×10^{12}	2650	5.7	9.8	187	51
A07	6×10^{11}	2300	5.6	10.2	−194	50
A15	1.45×10^{12}	1200	4.0	6.6	634	51
A16	6×10^{11}	690	3.2	4.5	1679	51
A17	4.8×10^{10}	530	2.2	3.2	1530	101
A35	Undoped	···	1.2	1.6	2163	100

sheet densities in the InGaAs wells of about 1×10^{12} cm^{-2} per well, as determined from Hall measurements. A summary of the structures investigated is given in Table I.

Intersubband absorption measurements are carried out using a Bio-Rad FTS-45A Fourier spectrometer with the samples in a 48° waveguide wedge geometry as described in Ref. 13. Figure 1(a) shows the room temperature absorption spectra of *p*-polarized incident light. (The *s* polarization shows essentially no absorption.) Intersubband transitions between the first and second subbands are measured for samples with well thicknesses from 3.2 to 10 nm and cover the spectral range from 5.6 to 12 μm (100–220 meV). As the well width is decreased, the E_1-E_2 transition energy gradually increases, reaching a maximum for well width of about 4 nm, and then again becomes smaller for well widths less than 4 nm as seen in Fig. 1. In our measurements, the width of the absorption peak is about 30 meV for samples with well width >4 nm, but was somewhat larger (41 meV) for the structure with the 3.2 nm wells and reduced transition energy. No absorption line was detected in sample A17 with 2.2 nm wells either because the wells are too narrow to allow a second subband or because the electron concentration is too low.

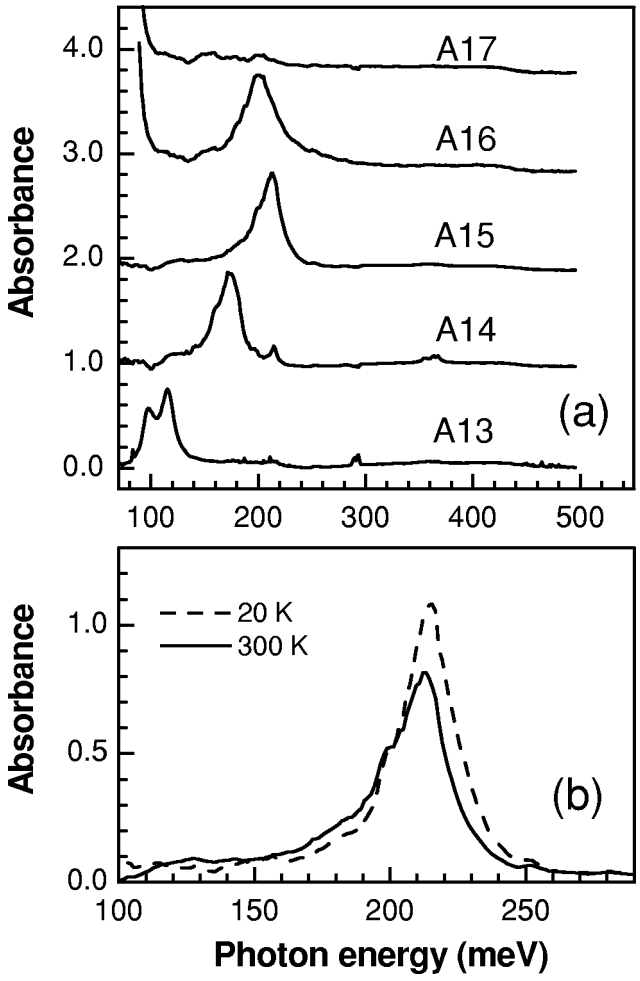

FIG. 1. (a) Room temperature midinfrared absorption spectra of the samples listed in Table I. The full width at half maximum for A13, A14, A15, and A16 are 29, 27, 28, and 41 meV, respectively. (b) Comparison of room temperature and low temperature absorption spectra for sample A15.

Figure 1(b) shows a comparison of absorption spectrum of sample A15 taken at 300 and 20 K. Beside the few millielectron volt blueshift, there is no other transformation of the line shape with decreased temperature. Such a temperature behavior of absorption spectrum is typical for highly doped superlattices.[14] Because first electron miniband around $k_{x,y}=0$ is fully occupied, there is no redistribution of electrons along k_z in momentum space at different temperatures.

To model the relationship between the band structure and the subband energies in our structures, we use the envelope function approximation model for superlattices.[15] Nonparabolicity of the conduction band is included by way of an energy dependent effective mass, as described in Ref. 16. The effect of strain on the conduction and valence bands is calculated following Van de Walle.[10] The conduction band offset ΔE_c is expected to be between 300 and 500 meV based on the model-solid theory (and corrected based on InGaP/GaAs experimental results[17,18]) and is treated as a fitting parameter. Interdiffusion at the heterointerfaces is included by adding a linearly graded $In_{0.32}Ga_{0.68}As_yP_{1-y}$ layer at each interface. The presence of a thin intermediate layer is consistent with preliminary high-resolution transmission electron microscopy investigations.[12] The interdiffusion layer thickness is a second fitting parameter and is necessary to allow the simultaneous fit of interband photoluminescence and intersubband absorption data.

Figure 2(a) depicts the calculated range of E_1-E_2 transition energies E_{1-2} as a function of well width for the $In_{0.32}Ga_{0.68}P/In_{0.32}Ga_{0.68}As$ superlattices listed in Table I together with the experimental positions of the interminiband absorption maxima. The top of the energy range corresponds to $k_z=0$ and the bottom to $k_z=\pi/d$, where d is the superlattice period. The doping level is sufficient to ensure that the Fermi level is always above the first electron miniband. The exact energy E_{1-2} is determined by using a line shape analysis of intersubband absorption[14] which indicates that the peak energy lies slightly above the E_1-E_2 transition at $k_z=\pi/d$ in the case of the ground electron miniband being filled. (The transition oscillator strength at $k_z=\pi/d$ dominates that at $k_z=0$ because the electron effective mass in the k_z direction is negative near the edge of the superlattice mini-Brillouin zone.[14]) Including the conduction band nonparabolicity, and As–P interdiffusion, the intersubband absorption data can be fit with a $\Delta E_c=400\pm50$ meV for realistic degrees of interdiffusion.

Requiring that the interband photoluminescence data also be fit further constrains the values of the two fitting parameters. Figure 2(b) shows the measured ground electron to heavy-hole state transitions for the investigated samples

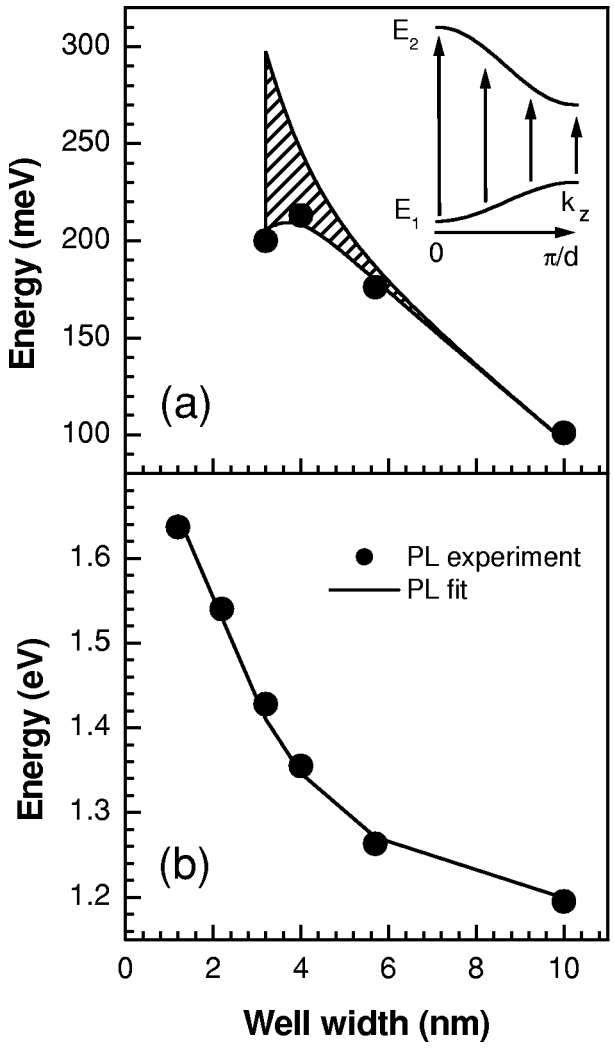

FIG. 2. (a) Energy of room temperature intersubband absorption maxima for samples A13–A16 and A07. The cross-hatched area is the range of the calculated E_1-E_2 transition energies for different k_z as described in the text. (b) Energies of the E_1-HH_1 transition energies determined from 10 K photoluminescence. The solid curve is the calculated E_1-HH_1 transition energy including As–P intermixing at the heterointerfaces.

together with calculated values again including nonparabolicity and interdiffusion. The values of the E_1-HH_1 transitions were determined from the low-temperature photoluminescence using the line shape analysis of Ref. 19. The simultaneous fit of both the intersubband absorption and the low-temperature photoluminescence is only possible for $\Delta E_c = 370$ meV and an interdiffusion of 1.4 monolayer per heterointerface.

The value of the electron effective mass at the bottom of the conduction band in the quantum wells is taken to be $m_e^*(\text{well}) = 0.060 m_0$ based on magnetoluminescence.[9] This value is also consistent with the measured value in strained $In_{0.2}Ga_{0.8}As$ of $0.063 m_0$[20] extrapolated to $y = 0.32$. The electron effective mass in the barrier material is taken to be $m_e^*(\text{barrier}) = 0.097 m_0$ and the heavy-hole mass was taken as $m_{hh}^* = 0.80 m_0$ in both materials. The fit is rather insensitive to $m_e^*(\text{barrier})$ and m_{hh}^*. As noted earlier, the nonparabolicity of the conduction band was included[16] and the resulting conduction band nonparabolicity parameters are 3.9 $\times 10^{-19}\text{m}^2$ in the wells and $1.5 \times 10^{-19}\text{m}^2$ in the barriers. The model calculation allows us to describe the intersubband transition energies in terms of the band alignment, strain- and energy-dependent effective masses, and interdiffusion in this heterojunction system. Thus, we expect to be able to use the same model with the same input parameters to design more complicated structures required for intersubband detectors and emitters.

To summarize, we have grown and studied strain-compensated $In_{0.32}Ga_{0.68}P/In_{0.32}Ga_{0.68}As$ superlattices with a high degree of internal strain, but on average lattice matched to GaAs. Intersubband transition energies between 100 and 220 meV have been demonstrated in this system. The intersubband absorption along with the low-temperature photoluminescence data are fit using a model incorporating the nonparabolicity of the conduction band, the effects of strain, and As–P interdiffusion. This investigation indicates that the conduction band edge discontinuity is about 370 meV, which is comparable to that of $Al_{0.45}Ga_{0.55}As/GaAs$. The present study provides a set of input parameters for calculating the band structure and emission or absorption energies in similar, but more complicated structures. These data further indicate that this strain-compensated system is an interesting candidate for applications based on intersubband emission or absorption such as quantum cascade lasers or quantum well infrared photodetectors.

The authors thank Dr. H. Kirmse for TEM measurements and discussion, J. Sölle for help with sample preparation, and they wish to acknowledge the support of the Deutsche Forschungsgemeinschaft within ''Forschergruppe 394.''

[1] R. Paiella, R. Martini, F. Capasso, C. Gmachl, H. Y. Hwang, D. L. Sivco, J. N. Baillargeon, A. Y. Cho, E. A. Whittaker, and H. C. Liu, Appl. Phys. Lett. **79**, 2526 (2001).
[2] B. F. Levine, J. Appl. Phys. **74**, R1 (1993).
[3] C. Sirtori, P. Kruck, S. Barbieri, P. Collot, J. Nagle, M. Beck, J. Faist, and U. Oesterle, Appl. Phys. Lett. **73**, 3486 (1998).
[4] G. Strasser, S. Gianordoli, W. Schrenk, E. Gornik, A. Mücklich, and M. Helm, J. Cryst. Growth **227–228**, 197 (2001).
[5] W.-S. Lour, Y.-W. Wu, S.-W. Tan, M-K. Tsai, and Y.-J. Yang, Appl. Phys. Lett. **80**, 3436 (2002).
[6] H. Page, C. Becker, A. Robertson, G. Glastre, V. Oritz, and C. Sirtori, Appl. Phys. Lett. **78**, 3529 (2001).
[7] L. R. Wilson, J. W. Cockburn, M. J. Steer, D. A. Carder, M. S. Skolnick, M. Hopkinson, and G. Hill, Appl. Phys. Lett. **78**, 413 (2001).
[8] C. Becker, C. Sirtori, H. Page, G. Glastre, V. Ortiz, X. Marcadet, M. Stellmacher, and J. Nagle, Appl. Phys. Lett. **77**, 463 (2000).
[9] M. Semtsiv, O. Bierwagen, F. Eickemeyer, G. G. Tarasov, and W. T. Masselink, Electronic Material Conference 2002.
[10] C. G. Van de Walle, Phys. Rev. B **39**, 1871 (1989).
[11] C. H. Yan and C. W. Tu, J. Cryst. Growth **164**, 276 (1996).
[12] H. Kirsme (private communication).
[13] F. Eickemeyer, R. A. Kaindl, M. Woerner, T. Elsaesser, S. Barbieri, P. Kruck, C. Sirtori, and J. Nagle, Appl. Phys. Lett. **76**, 3254 (2000).
[14] M. Helm, Semicond. Sci. Technol. **10**, 557 (1995).
[15] G. Bastard, Phys. Rev. B **24**, 5693 (1981).
[16] D. F. Nelson, R. C. Miller, and D. A. Kleinmann, Phys. Rev. B **35**, 7770 (1987).
[17] S. D. Gunapala, B. F. Levine, R. A. Logan, T. Tanbun-Ek, and D. A. Humphrey, Appl. Phys. Lett. **57**, 1802 (1990).
[18] W. T. Masselink, M. Zachau, T. W. Hickmott, and K. Hendrickson, J. Vac. Sci. Technol. B **10**, 966 (1992).
[19] S. K. Lyo and E. D. Jones, Phys. Rev. B **38**, 4113 (1988).
[20] G. Hendorfer, M. Seto, H. Ruckser, W. Jantsch, M. Helm, G. Brunthaler, W. Jost, H. Obloh, K. Köhler, and D. J. As, Phys. Rev. B **48**, 2328 (1993).